A New Inrush Detection Algorithm for Transformer Differential Protection

B. Kasztenny, N. Fischer, and Y. Xia
Schweitzer Engineering Laboratories, Inc.

Presented at the
12th International Conference on Developments in Power System Protection
Copenhagen, Denmark
March 31–April 3, 2014

A new inrush detection algorithm for transformer differential protection

B. Kasztenny*, N. Fischer*, Y. Xia*

**Schweitzer Engineering Laboratories, Inc., 2350 NE Hopkins Court, Pullman, WA 99163 USA, bogdan_kasztenny@selinc.com*

Keywords: Transformer differential protection, magnetizing inrush current, ultrasaturation, low second harmonic, dwell-time principle differential.

Abstract

Some power transformers, especially new designs with the core material improved for lower losses, produce low levels of second harmonic in their inrush magnetizing currents. Transformer differential relays face security problems when the second harmonic falls below the traditional 15 or 20 percent setting level. This paper derives a new protection method for detecting inrush conditions. The new algorithm is based on dwell-time periods in the inrush current. In each power cycle of a true inrush current, a period occurs where the differential current is both small and flat (dwell time). The new algorithm combines the absolute values of the instantaneous differential current with the absolute values of the differential current derivative to positively confirm both the low level and the flatness of the dwell-time currents. By utilizing the "flatness" feature of the waveshape, the algorithm performs well even under current transformer (CT) saturation. The new algorithm incorporates a separate method to cancel the inrush inhibit signal, allowing very fast operation for internal faults, particularly during inrush conditions. This dedicated element is based on a bidirectional instantaneous overcurrent principle.

1 Introduction

Power transformers rated above about 5 MVA are typically protected with differential (87T) elements against internal short circuits. The 87T differential signal is derived from the ampere-turn balance equations of the protected transformer [1]. As such, it responds to transformer faults and balances out to zero for load and external faults. Unfortunately, the 87T differential signal also responds to the transformer magnetizing current during inrush.

Transformer inrush currents can be large, in the order of five to seven times the transformer rated current, and they would normally cause the 87T element to misoperate if not properly blocked or restrained. Inrush currents are typically rich in harmonics, the second harmonic in particular. Therefore, the second-harmonic ratio in the differential currents has traditionally been used in transformer differential elements to block or to increase restraint of the differential elements during inrush conditions [2].

Some power transformers, especially those with new, improved core material designs for lower losses but also older units under some conditions [3], produce low levels of second harmonic in their magnetizing currents during energization. As a result, their 87T elements face security problems when the second harmonic falls below the traditional 15 or 20 percent setting level.

We show in this paper that low second harmonic is caused by deep saturation (ultrasaturation) of the transformer core. During ultrasaturation, the transformer core is subjected to very high levels of flux, and as a result, the core operating point traverses along the transformer magnetizing curve (B-H curve) in the saturated portion of the characteristic. This, in turn, makes the core appear more linear, as if it had only the saturated portion of the magnetizing curve. This linearity decreases the harmonic content in the inrush currents—sometimes well below 10 percent—causing security problems for transformer differential protection.

The paper explains ultrasaturation briefly and follows this explanation with a description of the new algorithm, based on analysis of the current waveshape, for detecting magnetizing inrush in transformers. The paper also describes a new method to accelerate tripping for internal faults during inrush conditions by canceling the standing inrush blocking signal. The new method is illustrated with field cases.

2 The problem of low second harmonic in transformer inrush currents

Cases of sporadic misoperation of transformer protection during inrush conditions are reported, with the common cause of the second-harmonic ratio being too low to properly block or restrain the differential element.

Fig. 1 shows a sample inrush current during relay misoperation due to a low second harmonic. The C-phase current is the largest, but it has a second-harmonic ratio well below 15 percent of the fundamental (Fig. 2), considered the lowest harmonic setting that does not impair dependability.

The level of the fourth harmonic is also low (about 2 percent in C-phase). Combining the second and fourth harmonics, such as using a harmonic restraining scheme, would not solve the problem either because the sum of the harmonic currents would still be below the 15 percent setting.

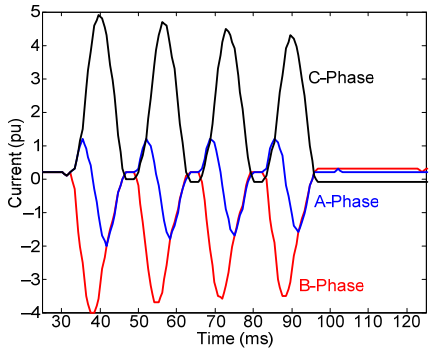

Fig. 1. Sample transformer terminal currents during energization.

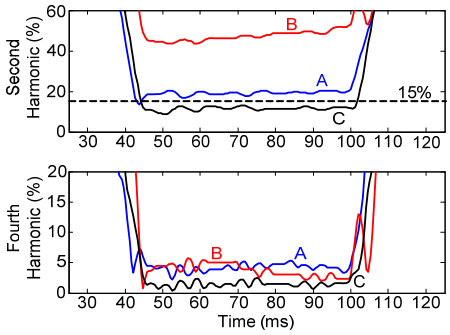

Fig. 2. Second- and fourth-harmonic ratios in the currents of Fig. 1.

When dealing with the challenge of low second harmonic, users are left with several solutions, including cross-phase blocking, lowering the second-harmonic threshold, or temporarily desensitizing the 87T elements upon transformer energization [3]. These solutions are not ideal because they could negatively impact the dependability of transformer protection.

As illustrated in Fig. 1, the magnetizing currents of a three-phase transformer (available as the differential signals to the 87T element) exhibit intervals where the currents are both small and flat. These periodic intervals last at least one-sixth of a power system cycle. We use this observation in our new algorithm for inrush detection.

3 Ultrasaturation in transformers

3.1 Explanation of ultrasaturation

The phenomenon of ultrasaturation can be explained by assuming a magnetizing characteristic with two linear regions, as shown in Fig. 3 and Fig. 4, and applying a sine-wave-shaped flux in the core with the magnitude below the saturation level while varying the amount of residual flux.

When the residual flux is near zero, the flux oscillates between the positive and negative saturation points and the transformer works in the linear region of the B-H curve, drawing only a very small excitation current. Assume next that the transformer is energized with some amount of residual flux, as shown in Fig. 3. The sine-wave flux is shifted in such a way that the maximum flux is on the second slope (saturated part) of the magnetizing characteristic, but the minimum flux is still below the positive saturation point. When the flux is above the saturation point, the transformer draws a large magnetizing current. When the flux is below the saturation point, the transformer draws a very small current. This switching between large and small magnetizing currents every power system cycle results in the typical shape of the inrush current with large values of the same polarity separated by periods of much smaller current (dwell-time periods), as shown in Fig. 1. The current is large, typically well above the transformer nominal current and the pickup setting of the 87T element.

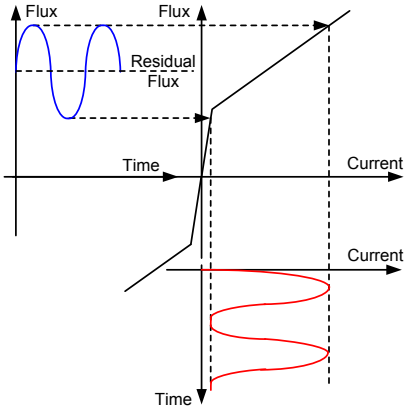

Fig. 3. Current and flux in the case when the minimum flux is close to the saturation level.

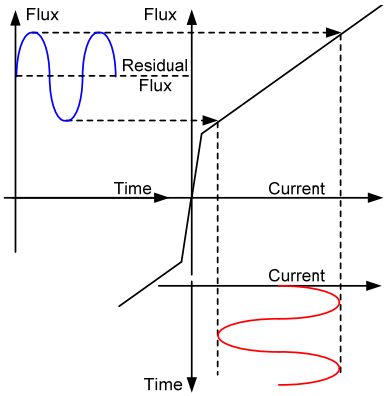

Fig. 4. Current and flux in the case when both the maximum and minimum flux values are above the saturation level.

Assume now that the residual flux increases so that the minimum flux is below the saturation level for only a very short period of time, as depicted in Fig. 3. In this case, the dwell-time periods are proportionally shorter and the current waveform appears closer to a sine wave, producing lower levels of harmonics.

Fig. 4 presents an extreme case when the flux is pushed above the saturation point so that even the minimum flux is above the saturation point. In this situation, the transformer draws a very large current, but the current waveform is not distorted and contains very little harmonics. The transformer core is operated in the saturated region of the B-H curve, but the magnetizing inductance, even though low, is constant, thereby yielding a current that is similar to a sine wave. This case is referred to as ultrasaturation [3] [4] [5].

Because the current waveform is relatively undistorted during ultrasaturation, the harmonic content is extremely low, thus jeopardizing the security of transformer differential protection.

References [3], [4], and [5] show that an aperiodic transient flux component during energization under an unfavorable combination of system conditions can shift the flux deeply into the saturation region.

Reference [3] shows that restrike of a switching device during transformer de-energization can build up the residual flux in the transformer core. The residual flux forces the flux into the ultrasaturation region, resulting in low levels of second harmonic.

3.2 Harmonics and dwell-time periods during ultrasaturation

Fig. 5 illustrates the second-harmonic content by plotting the percentage of second harmonic as a function of residual flux for the simplified cases shown in Fig. 3 and Fig. 4. When the residual flux increases slightly so that the transformer core starts saturating, the second-harmonic content increases considerably (Point A on the curve in Fig. 5). As the level of residual flux increases, the oscillating flux is pushed further into the saturation region, resulting in increased second-harmonic content (up to about 90 percent in our example). However, as the residual flux increases even more, the operating point of the flux versus current traverses greater portions of the second slope of the characteristic, resulting in a more sinusoidal shape of the current with decreasing second-harmonic content. The case of Fig. 3 results in roughly only 10 percent second-harmonic content (Point C in Fig. 5). The moment the oscillating flux is entirely pushed into the second slope region, the second harmonic decreases to extremely low values—eventually zero (Point D in Fig. 5).

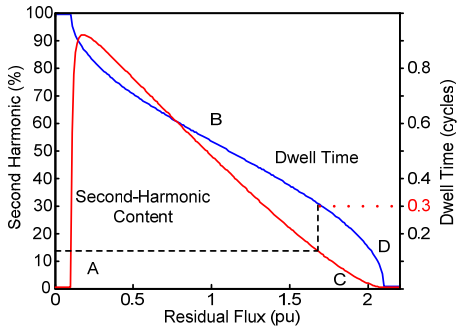

Fig. 5. Second-harmonic content (red) and duration of the dwell time (blue) as a function of residual flux.

Fig. 5 also shows the relationship between the level of residual flux and the duration of the dwell time. In this simulation, we define the dwell time as the fraction of a power system cycle during which the magnetizing current is below the saturation point. Therefore, when in linear operation (Point A), the dwell time is one full cycle. For moderate saturation (Point B), the dwell time is about half a cycle. For severe saturation (Point C), the dwell time is about 0.3 cycles. For ultrasaturation, the dwell time eventually reduces to zero, as expected (Point D and Fig. 4).

Importantly, Fig. 5 illustrates that the dwell time is a more robust criterion than the second harmonic. For example, when the second harmonic ratio drops below about 15 percent, the dwell time is still about 0.3 cycles. When the dwell time reduces to about one-sixth of a cycle, the second-harmonic content is below 10 percent.

3.3 Alignment of dwell-time periods in three-legged transformers

It is beneficial to notice that the dwell-time intervals are time-aligned between the three phases in the case of a three-phase, three-legged transformer (a prevailing design for economical and size reasons). In this design style, the flux in all three legs must sum to zero at any given time because the leakage flux is negligible. This is illustrated in Fig. 6.

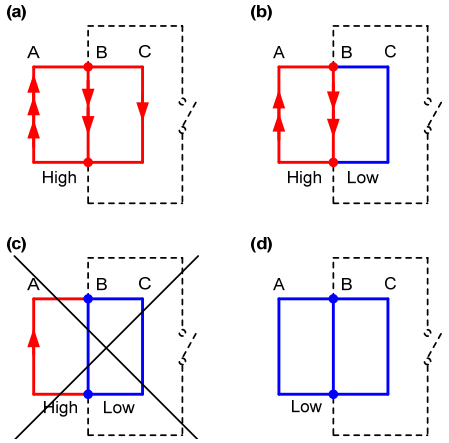

Fig. 6. Possible patterns of core saturation in a three-legged transformer design. The arrows represent flux. Red is high flux above the saturation level; blue is low flux below the saturation level; the dotted line represents the flux path through the air, oil, and tank.

Fig. 6a illustrates a period of time when the Leg A flux is so high that the returning flux in Legs B and C is also above the saturation level. In this case, all three legs are saturated and all three magnetizing currents are high (compare with Fig. 1).

Fig. 6b illustrates a period in time when the Leg A flux decayed to the point that the returning flux in Leg C is below the saturation level. As a result, the A and B flux values are equal and they must be of opposite directions. Comparing with Fig. 1, this period of time represents a situation where one magnetizing current is low and the two other magnetizing currents are still significant, equal in magnitude, and out of phase.

The situation of Fig. 6c is impossible. We cannot have a significant flux in Leg A with no flux in Legs B and C. Therefore, the case of Fig. 6b can only progress (as Leg A pulls further out of saturation) into the case of Fig. 6d. This means that as Leg A pulls out of saturation, the companion Leg B pulls out of saturation as well. As a result, all three legs are out of saturation at the same time. Comparing with Fig. 1, this is a period of time when all three currents are near zero.

Because the transformer is energized from a symmetrical ac source, the pattern of Fig. 6a, b, and d keeps repeating

(see Fig. 1). In particular, the situation of Fig. 6d (all currents are near zero at the same time) is guaranteed to repeat itself every power system cycle.

We use the fact that all three currents exhibit their dwell times at the same time in our algorithm for three-legged transformers.

The situation is different in single-phase units or four- and five-legged cores. In these cases, the dwell-time intervals appear independent in each phase because the fluxes in all the single-phase cores are independent and the fourth and fifth legs provide independent return paths for the flux in the four- and five-legged transformers.

4 A new method to address inrush during ultrasaturation

This section describes an improved inrush detection algorithm based on the dwell-time principle: the existence of periods of small and flat currents in every cycle of a true inrush current.

4.1 A new dwell-time-based algorithm

Fig. 7 presents a simplified block diagram of the new inrush detection algorithm for three-legged transformers. Instantaneous values of the phase differential currents (87T IDIF A, 87T IDIF B, and 87T IDIF C) are the inputs to the algorithm, and the Boolean output INRUSH is the output (when asserted, the differential element shall be blocked). The algorithm uses information from all three phases but asserts a single output.

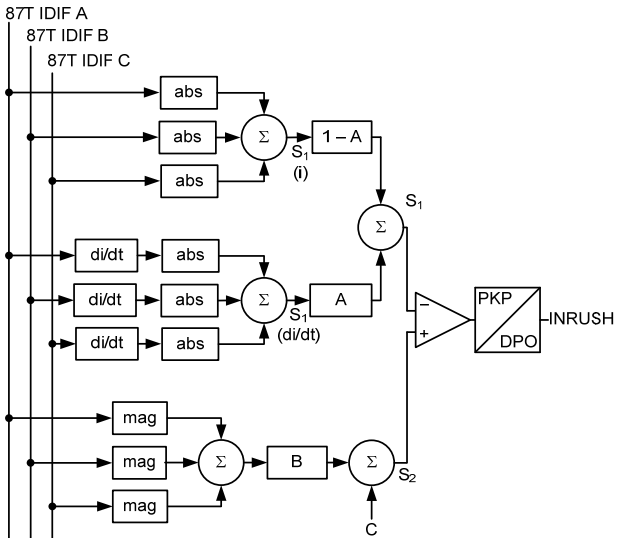

Fig. 7. Simplified block diagram of the new inrush detection algorithm.

The algorithm is executed on a sample-by-sample basis and works as follows:

- The absolute values of the instantaneous differential currents in all three phases are added to form the S_1 (i) signal. During inrush conditions, this signal is very low for the duration of the dwell-time periods because all three differential currents exhibit their dwell times at the same time. During internal fault conditions, this signal is high and reflects the fault current. If current transformer (CT) saturation occurs during inrush, the differential currents during dwell-time periods start departing from zero and S_1 (i) starts to increase slightly with time.
- The instantaneous differential signals are differentiated (di/dt). Because the inrush currents are flat during dwell-time periods, the result of the derivative is ideally zero. The absolute values of the derivatives are calculated next, and all three phases are summed to form the S_1 (di/dt) signal. Because all three inrush currents are flat during the dwell-time periods, this signal is very low during inrush conditions for the duration of the dwell-time periods. If CTs saturate during inrush, this signal may increase as well, but at a much lower rate compared with the S_1 (i) signal.
- The S_1 (i) and S_1 (di/dt) signals are added using the weighting factor A (for the purpose of demonstration, a value of $A = 0.5$ is used). The resulting signal S_1 is low during the dwell-time periods of the inrush and high during internal faults. This signal is quite resilient to CT saturation during inrush. We can further increase the resilience of the algorithm to CT saturation during inrush by increasing the value of A.
- The magnitudes of the phase differential currents are measured and added together. S_2 is formed as a portion of the sum of the magnitudes (multiplier B) plus a constant, C. For the purpose of demonstrating the algorithm operation, B is 0.1 and C is 0.1 of the transformer rated current.
- During inrush, the S_1 signal is very low once a cycle for the duration of the dwell time. The comparator checks the level of S_1. If this signal is low for the duration of the pickup time (PKP), then INRUSH is asserted and maintained for the DPO time (typically one power system cycle). The dropout timer is required to wait for the next dwell-time period in order to maintain reliable inrush detection.
- The pickup timer (PKP) is set to the desired level of dependability in detecting inrush. For example, it can be set to one-sixth (or even as low as one-eighth) of the power cycle, allowing it to cope with cases of the second harmonic as low as 10 percent and below (see Fig. 5).

Fig. 8 through Fig. 10 illustrate operation of the new algorithm using an inrush case recorded in the field with a simulated fault current superimposed on the inrush waveform (in Fig. 8, the fault was added at about 72 milliseconds). This case is a realistic representation of an internal fault that develops during transformer energization. We expect the algorithm to block for the first 72 milliseconds of inrush (protection security) and deassert shortly afterward (protection dependability).

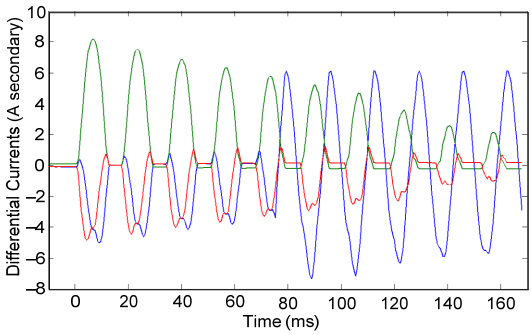

Fig. 8. Differential currents for an internal fault during inrush conditions.

Fig. 9 shows some key internal signals of the algorithm. As expected during inrush conditions, the S_1 (i), S_1 (di/dt), and S_1 signals are low for the duration of the dwell-time periods. After the internal fault develops in the blue phase, the dwell-time intervals have practically disappeared from the S_1 signal, though the other two phases continue to look like true inrush currents with clearly visible dwell-time periods.

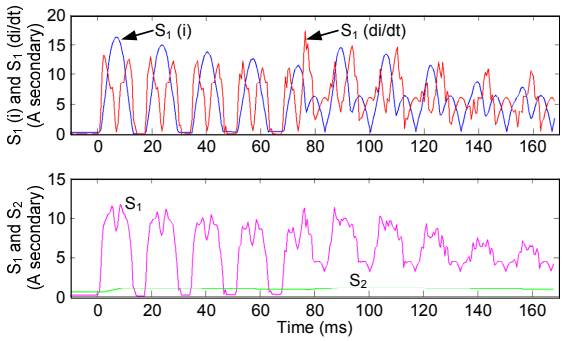

Fig. 9. S_1 (i) (blue), S_1 (di/dt) (red), S_1 (magenta), and S_2 (green) signals for the case of Fig. 8.

The S_1 signal drops repetitively below the S_2 signal during inrush and stays consistently above the S_2 signal after the internal fault (Fig. 9). This means that during inrush conditions, the PKP timer picks up and maintains a solid INRUSH assertion. The last dwell-time interval in the S_1 signal occurs at about 65 milliseconds. If it was not for the internal fault, the next interval would occur at about 65 + 17 = 82 milliseconds. The DPO timer expires after about one cycle (around 82 milliseconds), and because there is no new dwell-time period present, INRUSH deasserts, allowing the differential element to trip.

When applied to single-phase units, the scheme needs to be phase-segregated [i.e., using the phase-segregated signals S_1 (i), S_1 (di/dt), S_1, and S_2]. This is because the dwell-time intervals are not aligned in time in single-phase or four- or five-legged core design transformers.

The new scheme is simple and intuitive. It does not require any user settings because the four design constants (*A*, *B*, *C*, and PKP timer) can be selected for a wide range of transformers. Of these factory constants, only the PKP time may be of some interest to users because it determines the balance between protection security (short delay equals declaring inrush for short dwell times) and dependability (longer delay equals declaring a fault if dwell times are too short).

The new scheme improves the performance of previous implementations of the dwell-time principle by using a derivative of the current in addition to the current itself (to improve performance for CT saturation) and by correlating information from all three phases. Requiring that all three phases simultaneously display their dwell intervals increases security of the inrush detection scheme (i.e., prevents it from declaring an inrush during internal faults with heavy CT saturation). It is important to notice that the method is not a cross-phase blocking method: if any of the phases stop exhibiting dwell times, the scheme deasserts (see Fig. 9).

The scheme shares, however, one common disadvantage with traditional second-harmonic blocking applications—it takes approximately one cycle to deassert the blocking signal after an internal fault during inrush. In the case of second-harmonic blocking, the delay results from the transient response of the second-harmonic filters. In the new method, the delay is intentional and set by the DPO timer of about one cycle.

4.2 Bidirectional differential overcurrent element

The inrush current, if high, is practically unipolar. It becomes more symmetrical as the inrush decays into a steady-state excitation current.

Fig. 10 shows the B-phase differential current of Fig. 8 superimposed onto two thresholds. During inrush conditions (the first 72 milliseconds), the differential current is negative and repeatedly crosses the negative threshold (the dashed blue line in Fig. 10). At the same time, however, it does not cross the symmetrically placed positive threshold (the dashed red line).

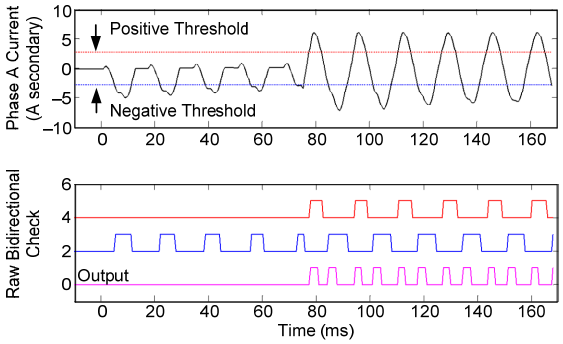

Fig. 10. B-phase differential current of Fig. 8 compared with positive (red) and negative (blue) thresholds. The magenta signal represents the output of the bidirectional overcurrent element.

However, when the internal fault happens, the current crosses the negative threshold; shortly afterwards, it crosses the positive threshold; and so on. We use this observation to devise a new protection element as depicted in Fig. 11.

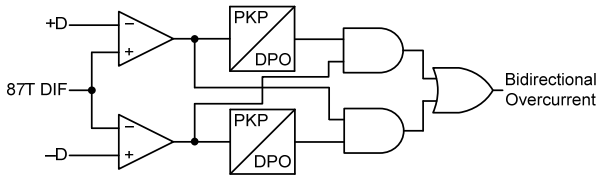

Fig. 11. Principle of operation of the bidirectional differential overcurrent element.

In this scheme, the instantaneous differential current (87T DIF) is compared with the positive (+D) and negative (–D) thresholds. If the differential current is above the positive threshold for a short duration of time (PKP timer), a window, equal to the DPO timer, is opened to check if the current decreases to below the negative threshold. If it does, the current must be symmetrical, and therefore, it is not an inrush current. Mirror logic is used for the negative polarity—if the current is confirmed significantly negative and shortly afterward it becomes positive, the inrush hypothesis is ruled out.

The PKP timer in Fig. 11 is introduced for security (one-eighth of a cycle, for example). The DPO timer is set to about one-third to one-half of a cycle.

The magenta line in Fig. 10 is the output of the bidirectional overcurrent element. As we can see, the element asserts at about 78 milliseconds (the fault occurred at about 72 milliseconds). This response time of about 6 milliseconds to a fault occurring during inrush is considerably faster compared with the reset time of about one cycle of any inrush detection method (second-harmonic blocking or the new method presented in the previous subsection).

Owing to the bidirectional level check, this element does not have to be set very high to ensure security during inrush or external faults with CT saturation. As a result, it has a chance to respond to a larger percentage of internal faults compared with the traditional unrestrained differential element.

4.3 Application considerations

The new method of detecting inrush conditions can be used alone, or it can be combined with either harmonic blocking or harmonic restraining.

The new bidirectional instantaneous differential overcurrent element can be applied to unblock the differential element with the intent to accelerate the operation of the traditional differential element, or it can be used directly for tripping in a manner similar to the traditional unrestrained differential element (see Fig. 12). The direct tripping application [Bidirectional Overcurrent (2) initiating a trip without any through-fault restraint or harmonic blocking] may use slightly higher settings for security, but it still can be set much more sensitive compared with the element that responds to the filtered magnitude of the differential current.

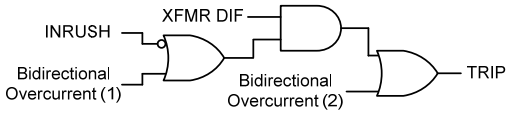

Fig. 12. Applications of the new elements.

5 Conclusion

This paper reviews magnetizing inrush conditions in power transformers. Special emphasis is put on the cases of ultrasaturation when not only the maximum but also the minimum flux is near or above the transformer core saturation point.

Deep saturation results in lower levels of second harmonic in the differential currents and can lead to the misoperation of transformer differential relays due to insufficient harmonic blocking or restraining.

A new method is presented based on the dwell-time principle, using information from all three phases as well as the derivative of the differential current. The new method allows blocking of the differential elements for very deep core saturation without jeopardizing protection dependability. As such, the new method is considerably better than the second-harmonic principle. Also, it is more resilient to CT saturation during either magnetizing inrush or internal faults.

The bidirectional instantaneous differential overcurrent element allows faster inrush unblocking. It can also be used for direct tripping. The element can operate in half a cycle, even at relatively low internal fault current levels.

References

[1] B. Kasztenny, M. Thompson, and N. Fischer, "Fundamentals of Short-Circuit Protection for Transformers," proceedings of the 63rd Annual Conference for Protective Relay Engineers, College Station, TX, March 2010.

[2] A. Guzmán, H. Altuve, and D. Tziouvaras, "Power Transformer Protection Improvements With Numerical Relays," proceedings of the CIGRE B5 Colloquium, Calgary, Canada, September 2005.

[3] S. Hodder, B. Kasztenny, N. Fischer, and Y. Xia, "Low Second-Harmonic Content in Transformer Inrush Currents – Analysis and Practical Solutions for Protection Security," proceedings of the 40th Annual Western Protective Relay Conference, Spokane, WA, October 2013.

[4] X. N. Lin and P. Liu, "The Ultra-Saturation Phenomenon of Loaded Transformer Energization and Its Impacts on Differential Protection," *IEEE Transactions on Power Delivery*, Vol. 20, Issue 2, April 2005, pp. 1265–1272.

[5] A. Wiszniewski, W. Rebizant, D. Bejmert, and L. Schiel, "Ultrasaturation Phenomenon in Power Transformers—Myths and Reality," *IEEE Transactions on Power Delivery*, Vol. 23, Issue 3, July 2008, pp. 1327–1334.

Previously presented at the 12th International Conference on Developments in Power System Protection.